TABLE IX. Ground-state properties of diamond, Si, and Ge: lattice constant, a; cohesive energy, E_c; and bulk modulus B.

	a (a.u.)	E_c (eV)	B (Mbar)
	Diamond		
Experiment[a]	6.740	7.37	4.43
ASA-HL[b]	6.67	8.5	4.90
pseud-W[c]	6.807	7.58	4.33
ASA-BH[d]	6.709	8.43	4.64
BH[e]	6.744		4.42
	Silicon		
Experiment[a]	10.26	4.63	0.99
ASA-HL[b]	10.22	4.8	0.98
pseud-W[c]	10.30	4.84	0.98
ASA-BH[d]	10.29	4.94	0.95
pseud-CA[f]	10.20	5.28	0.94
	Germanium		
Experiment[g]	10.68	3.85	0.770
ASA-HL[b]	10.78	3.6	0.660
pseud-W[c]	10.69	4.02	0.730
pseud-CA[f]	10.58	4.67	0.730

Phys. Rev. B 59, 1758 (1999)

Rev. Mod. Phys. 61, 689 (1989)

TABLE V. Comparison of the equilibrium lattice constant (a), bulk modulus (B), and magnetic moment (M_0) for bcc FM Fe, hcp NM Fe, hcp FM Co, and fcc FM Ni calculated with PAW, US-PP, and FLAPW scalar relativistic calculations (the GGA results are in parentheses).

		a (Å)	B (Mbar)	M_0 (μ_B)
bcc Fe	FLAPW[a]	2.76 (2.83)	2.45 (1.89)	2.04 (2.17)
(FM)	PAW	2.75 (2.83)	2.47 (1.74)	2.00 (2.20)
	US-AE	2.75 (2.83)	2.45 (1.75)	2.01 (2.19)
	US-PP	2.76 (2.85)	2.37 (1.51)	2.08 (2.32)
hcp Fe	FLAPW[a]	2.38 (2.43)	3.44 (2.91)	
(NM)	PAW	2.38 (2.43)	3.46 (2.85)	
	US-AE	2.38 (2.43)	3.46 (2.82)	
	US-PP	2.38 (2.43)	3.38 (2.78)	
hcp Co	PAW	2.43 (2.49)	2.73 (2.13)	1.51 (1.59)
(FM)	US-PP	2.43 (2.50)	2.67 (2.07)	1.52 (1.62)
fcc Ni	FLAPW[b]	(3.52)	(2.00)	(0.60)
(FM)	PAW	3.43 (3.52)	2.51 (1.94)	0.58 (0.61)
	US-PP	3.44 (3.53)	2.48 (1.94)	0.56 (0.62)

Spin density functional theory

Kohn-Sham formulation of DFT

$$[-\frac{\hbar^2}{2m}\nabla^2 + v(\mathbf{r}) + \int \frac{n(\mathbf{r}')}{|\mathbf{r}-\mathbf{r}'|}d\mathbf{r}' + \frac{\delta E_{XC}}{\delta n(\mathbf{r})}]\phi_i(\mathbf{r}) = \epsilon_i\phi_i(\mathbf{r})$$

$$n(\mathbf{r}) = \sum_{i=1}^{N} |\phi_i(\mathbf{r})|^2$$

Generalization to spin DFT (Barth & Hedin (1972))

2x2 spin-density matrix

$$n_{\alpha\beta}(\mathbf{r}) = \sum_{i=1}^{N} \phi_i^{*\alpha}(\mathbf{r})\phi_i^{\beta}(\mathbf{r})$$

$$\underline{\mathrm{n}}(\mathbf{r}) = \frac{1}{2}(n(\mathbf{r})\mathrm{I} + \sigma\cdot\mathbf{m}(\mathbf{r}))$$

$$= \frac{1}{2}\begin{pmatrix} n(\mathbf{r}) + m_z(\mathbf{r}) & m_x(\mathbf{r}) - im_y(\mathbf{r}) \\ m_x(\mathbf{r}) + im_y(\mathbf{r}) & n(\mathbf{r}) - m_z(\mathbf{r}) \end{pmatrix}$$

Spin density functional theory (contd.)

Similarly, potential matrices are written as

$$\underline{\mathrm{v}}(\mathbf{r}) = v(\mathbf{r})\mathrm{I} + \mu_B \sigma \cdot \mathbf{B}(\mathbf{r})$$

$$\underline{\mathrm{v}}_{\mathrm{XC}}(\mathbf{r}) = v_{\mathrm{XC}}(\mathbf{r})\mathrm{I} + \mu_B \sigma \cdot \mathbf{B}_{\mathrm{XC}}(\mathbf{r})$$

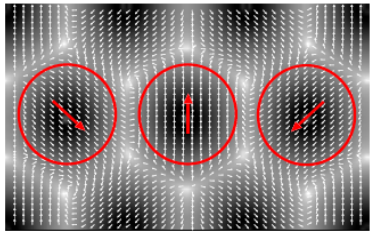

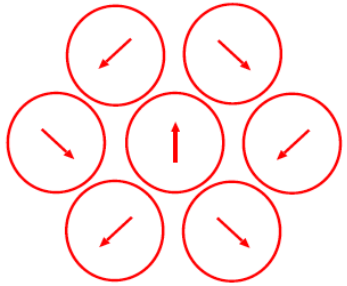

Magnetic ground state of hexagonal Cr monolayer

For collinear case

$$(\frac{\hbar^2}{2m}\nabla^2 + v_{Coul}(\mathbf{r}) + B_z(\mathbf{r}) + v^{\uparrow}_{XC}(\mathbf{r}))\phi^{\uparrow}_i(\mathbf{r}) = \epsilon^{\uparrow}_i \phi^{\uparrow}_i(\mathbf{r})$$

$$(\frac{\hbar^2}{2m}\nabla^2 + v_{Coul}(\mathbf{r}) - B_z(\mathbf{r}) + v^{\downarrow}_{XC}(\mathbf{r}))\phi^{\downarrow}_i(\mathbf{r}) = \epsilon^{\downarrow}_i \phi^{\downarrow}_i(\mathbf{r})$$

Performance of DFT
Comparison between theory and experiment

Property	source	Fe (bcc)	Co (fcc)	Ni (fcc)	Gd (hcp)
M_{spin}	LSDA	2.15	1.56	0.59	7.63
M_{spin}	GGA	2.22	1.62	0.62	7.65
M_{spin}	experiment	2.12	1.57	0.55	
$M_{tot.}$	experiment	2.22	1.71	0.61	7.63

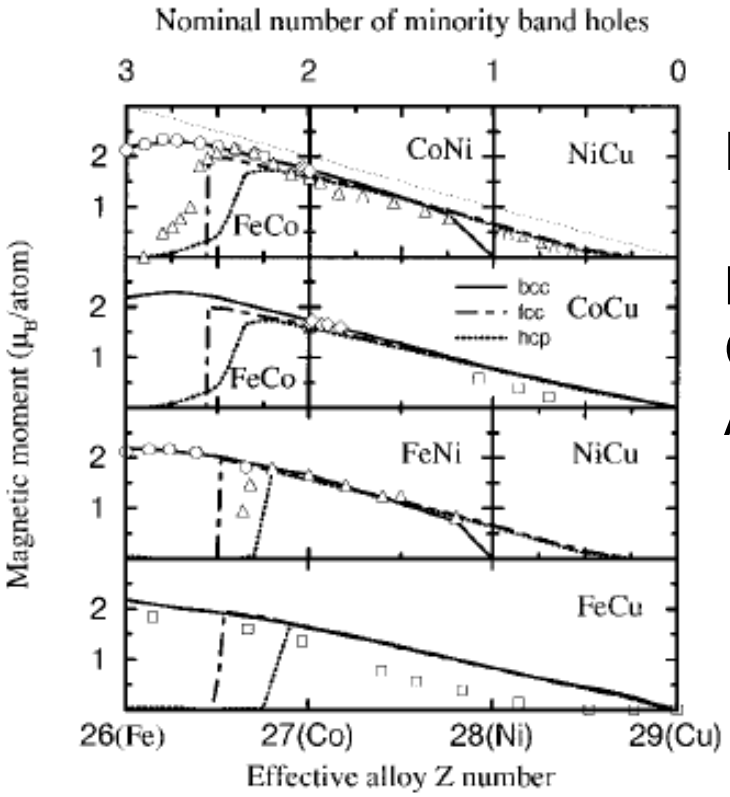

Random binary alloys

LMTO +
Coherent Potential
Approximation (CPA)

PRB **59**, 419 (1999)

Basis sets:
diverse electronic structure methods

- Gaussian (GAUSSIAN, CRYSTAL,……)
- Plane wave (VASP, CASTEP, QUANTUM ESPRESSO, ABINIT,…….)
- Localized orbitals (SIESTA, FPLO,……..)
- Linearized muffin tin orbital (Stuttgart LMTO, Uppsala Rspt,……)
- Linearized augmented plane wave (ELK, EXCITING, WIEN2K, FLEUR,….)
- ……..
- ……..
- ……

Periodicity, Bloch's theorem & plane waves

$$\psi_{n,\mathbf{k}}(\mathbf{r}+\mathbf{R}) = \psi_{n,\mathbf{k}}(\mathbf{r})e^{i\mathbf{k}.\mathbf{R}}$$ Bloch's theorem

$$\psi_{n,\mathbf{k}}(\mathbf{r}) = u_{n,\mathbf{k}}(\mathbf{r})e^{i\mathbf{k}.\mathbf{r}}$$

$$u_{n,\mathbf{k}}(\mathbf{r}) = \Omega^{-1/2}\sum_{\mathbf{G}} C_{\mathbf{G}n\mathbf{k}}e^{i\mathbf{G}.\mathbf{r}}$$

$$\psi_{n,\mathbf{k}}(\mathbf{r}) = \Omega^{-1/2}\sum_{\mathbf{G}} C_{\mathbf{G}n\mathbf{k}}e^{i(\mathbf{G}+\mathbf{k}).\mathbf{r}}$$

$$\rho(\mathbf{r}) = \sum_{\mathbf{G}} \rho_{\mathbf{G}}e^{i\mathbf{G}.\mathbf{r}}, V(\mathbf{r}) = \sum_{\mathbf{G}} V_{\mathbf{G}}e^{i\mathbf{G}.\mathbf{r}}$$

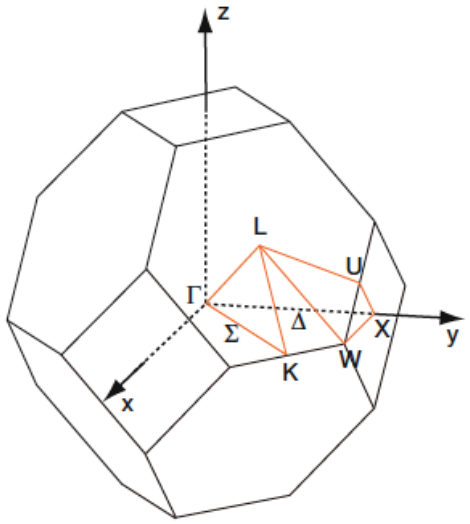

Brillouin zone: fcc lattice

Only the plane waves |**G**+**k**> are included for which

$$\frac{\hbar^2}{2m_e}|\mathbf{G}+\mathbf{k}|^2 < E_{cutoff}$$

Pseudopotentials

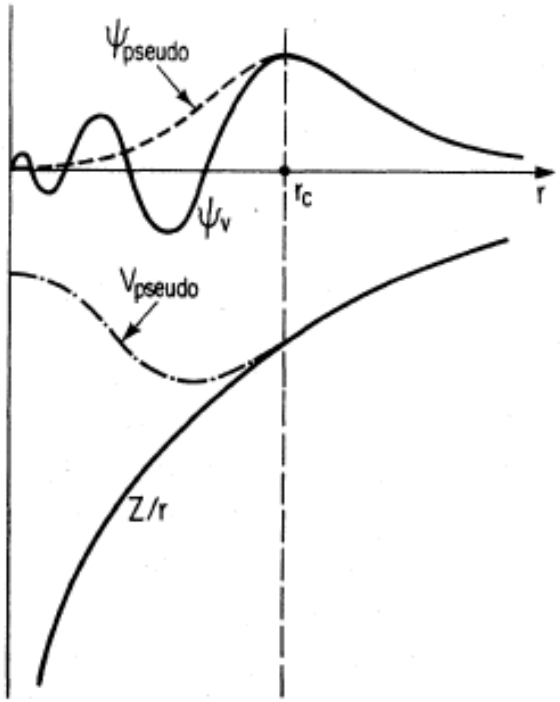

Norm conserving pseudopotential
Ultrasoft pseudopotential
Projector Augmented Wave

Projector Augmented Wave (PAW)

$$|\psi_n\rangle = |\tilde{\psi}_n\rangle + \sum (|\phi_{lm\varepsilon}\rangle - |\tilde{\phi}_{lm\varepsilon}\rangle)\langle \tilde{p}_{lm\varepsilon} | \tilde{\psi}_n\rangle$$

$$\langle \tilde{p}_{lm\varepsilon} | \tilde{\phi}_{l'm'\varepsilon'}\rangle = \delta_{ll'}\delta_{mm'}\delta_{\varepsilon\varepsilon'}$$

$$c_{lm\varepsilon} = \langle \tilde{p}_{lm\varepsilon} | \tilde{\psi}_n\rangle$$

$$|\psi_n\rangle = |\tilde{\psi}_n\rangle - \sum |\tilde{\phi}_{lm\varepsilon}\rangle c_{lm\varepsilon} + \sum |\phi_{lm\varepsilon}\rangle c_{lm\varepsilon}$$

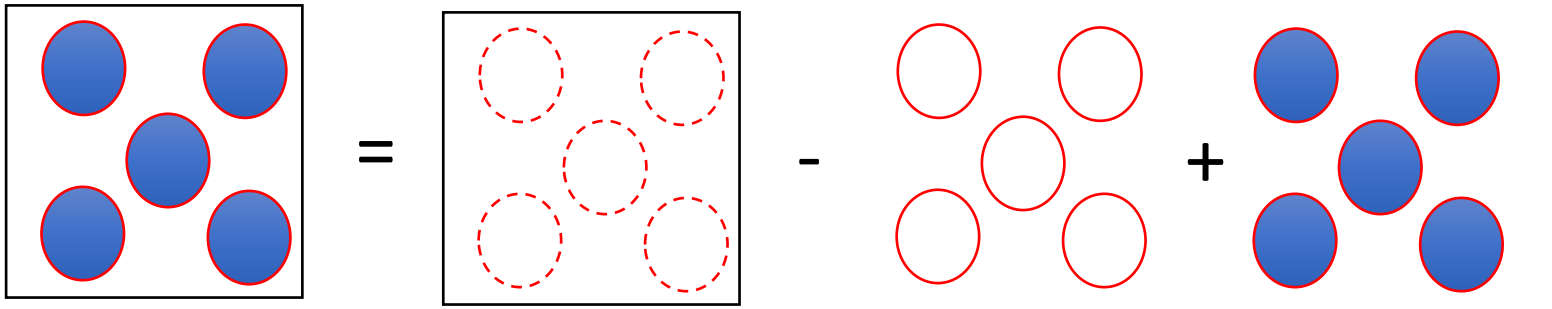

Muffin tin approximation

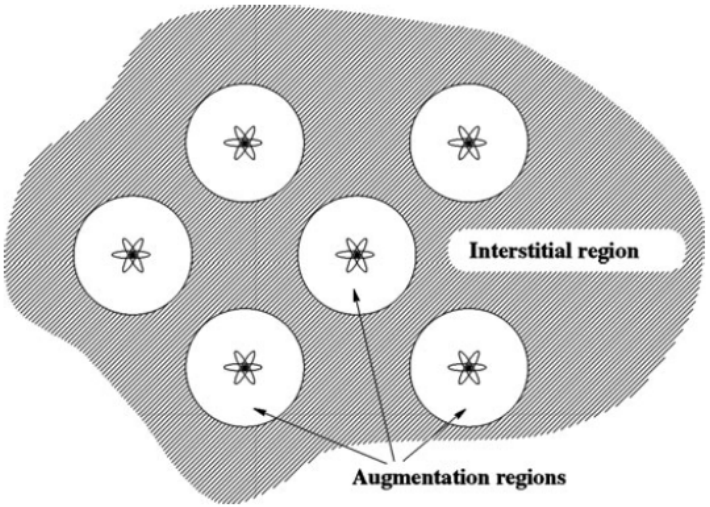

$$V(r) = \sum_R v(|\boldsymbol{r} - \boldsymbol{R}|)\theta(S - |\boldsymbol{r} - \boldsymbol{R}|)$$

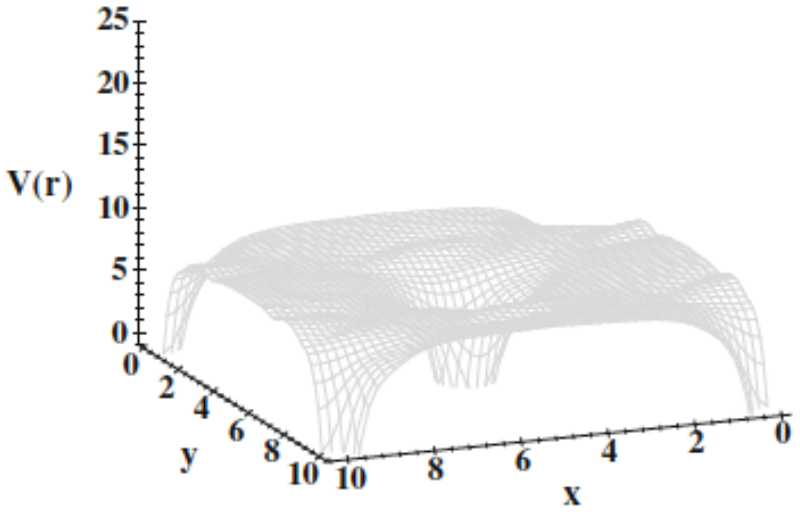

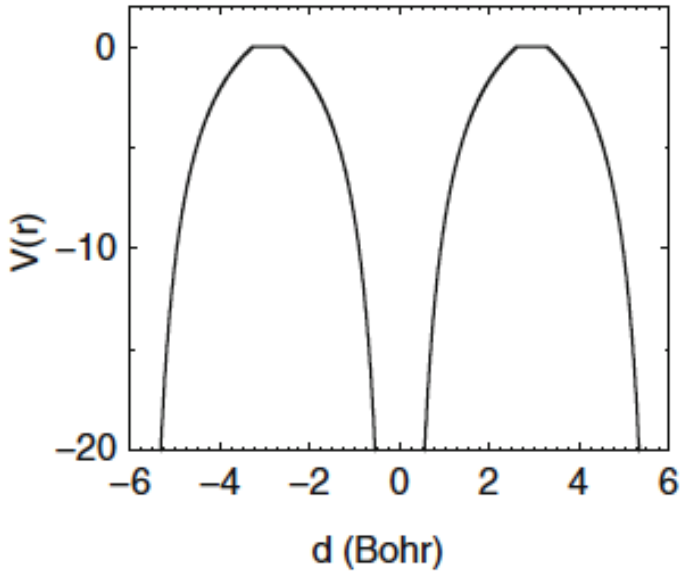

Augmented Planewave (APW) Method

•J.C. Slater, *Phys. Rev.* **51**, 846 (1937); *Phys. Rev.* **81**, 385 (1951).

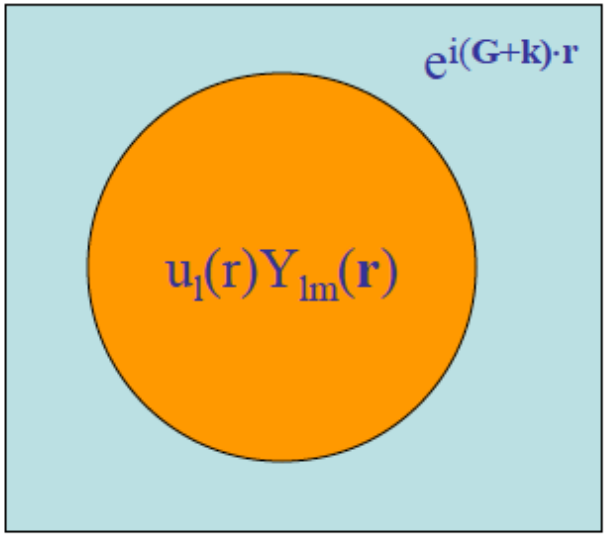

Divide Space Into 2 Regions:

- Atom Centered Spheres
- Interstitial

"Basis" Consists of Planewaves in the Interstitial and Radial Functions in the Spheres.

$$\varphi(\mathbf{r}) = \begin{cases} \Omega^{-1/2} \sum_{\mathbf{G}} c_{\mathbf{G}}\, e^{i(\mathbf{G}+\mathbf{k})\cdot\mathbf{r}} & \mathbf{r} \in \text{Interstitial (I)} \\ \sum_{lm} A_{lm}\, u_l(r)\, Y_{lm}(\mathbf{r}) & \mathbf{r} \in \text{Sphere (S)} \end{cases}$$

- $u_l(r)$ are the radial solutions of Schrodinger's equation at the energy of interest (i.e. the band energy).

The Linearized Augmented Planewave (LAPW) Method

O.K. Andersen, Phys. Rev. B **12**, 3060 (1975).

Key Ideas:

- The problem with the APW method is the energy dependence of the secular equation which is a result of the energy dependence of the augmenting function.
- Solution: Add variational freedom: particularly $\mathring{u}(r) = \partial u(r)/\partial E$.

$$\varphi(\mathbf{r}) = \begin{cases} \Omega^{-1/2} \sum_{\mathbf{G}} c_{\mathbf{G}}\, e^{i(\mathbf{G}+\mathbf{k})\cdot\mathbf{r}} & \mathrm{r}\in\mathrm{I} \\ \sum_{lm} \left(A_{lm}\, u_l(\mathrm{r}) + B_{lm}\, \mathring{u}_l(\mathrm{r})\right) \mathrm{Y}_{lm}(\mathbf{r}) & \mathrm{r}\in\mathrm{S} \end{cases}$$

- Where A_{lm} ***and*** B_{lm} are determined by matching the value and derivative of the basis functions at the sphere boundary.

Multiple scattering theory

Korringa-Kohn-Rostoker (KKR) method

1) Two aspects need to be considered
   (a) structure (position of atoms)
   (b) scattering (chemical identity)
2) Green function approach:
   suitable for random alloys, disordered systems in general, surfaces, impurities, response functions, transport etc.)

$G(\mathbf{r}, \mathbf{r}', E)$: propagation of an electron from site **r** to **r'** with energy E

Dyson equation

$$G = G_0 + G_0 t G_0 + G_0 t G_0 t G_0 + ...$$
$$= G_0 + G_0 t G$$

G_0 : free propagator without any scattering in between

t : single-site scattering matrix

The Green function can be written as

$$G = (G_0^{-1} - t)^{-1}$$

One can define the scattering path operator (full multiple scattering matrix for the entire system) as

$$T = (t^{-1} - G_0)^{-1}$$

Condition of stationary states (leading to the eigenvalues)

$$det[t_l^{-1}(E, \mathbf{R})\delta_{\mathbf{R}\mathbf{R}'}\delta_{LL'} - G_{0LL'}(E, \mathbf{R} - \mathbf{R}')] = 0$$

(scattering matrix: chemical identity) (structure constant matrix: geometry)

For ordered systems, use reciprocal space representation: Fourier transform of G_0

Density of states (DOS) is calculated as

$$n(E) = -\frac{1}{\pi} Im \int d\mathbf{r} G(\mathbf{r}, \mathbf{r}, E)$$

Relationship between Bloch spectral density and DOS

$$n(E) = \frac{1}{\Omega_{BZ}} \int_{\Omega_{BZ}} d\mathbf{k} A_B(\mathbf{k}, E)$$

Results of DFT calculations

Convergence of total energy

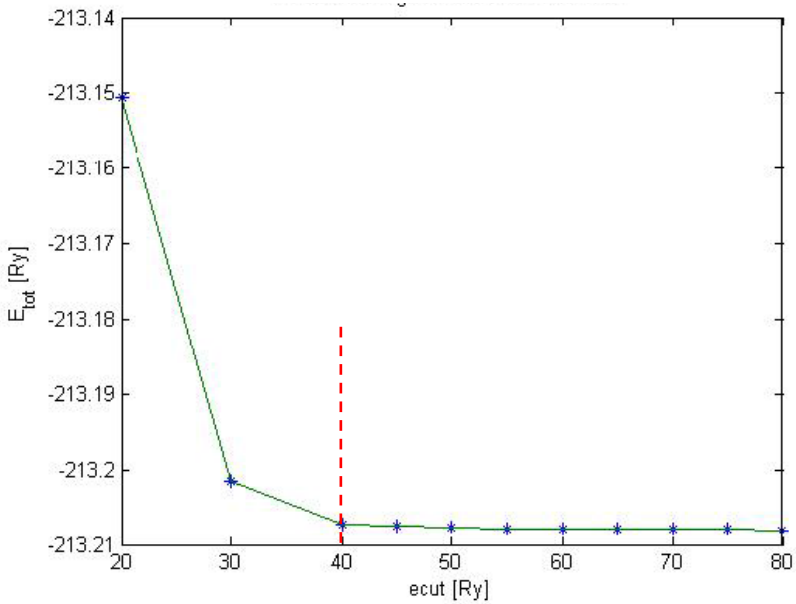

Figure 3: Total energy vs. ecut for fcc Cu

$$\frac{\hbar^2}{2m_e}\left|\mathbf{G}+\mathbf{k}\right|^2 < E_{cutoff}$$

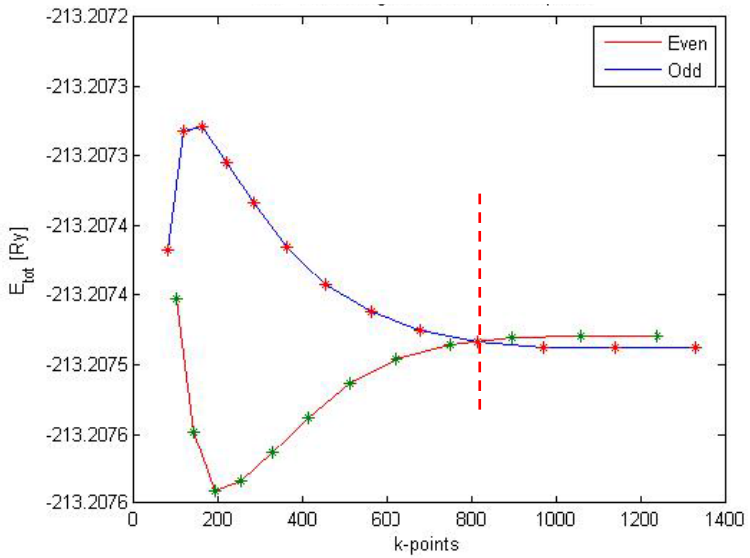

Figure 4: Total energy vs. number of k-points for fcc Cu

Results of DFT calculations (contd.)

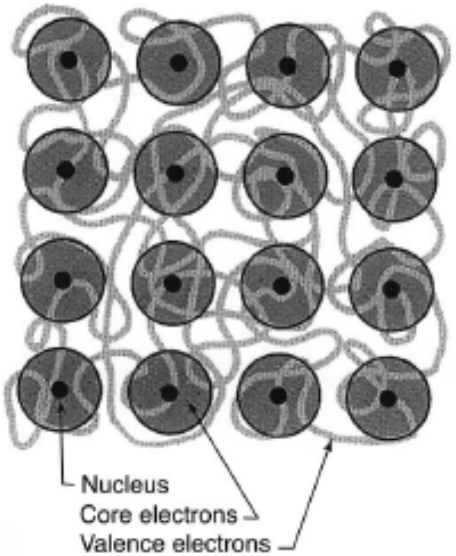

Band structure: fcc Cu

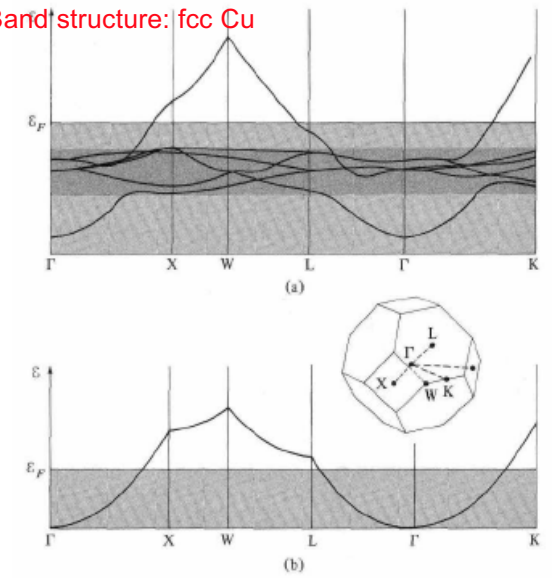

Density of states: fcc Cu

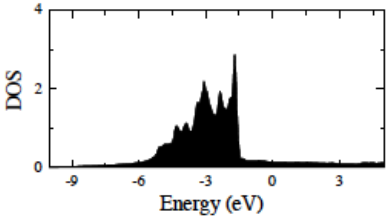

Stability of structural phases

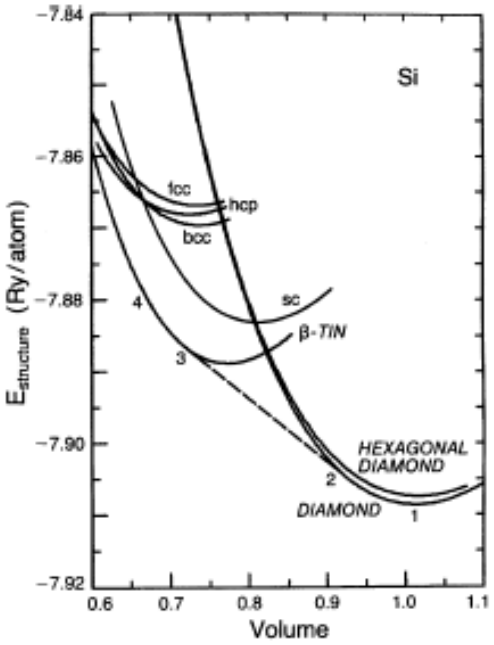

Band structure
Expt: ARPES

Density of states:
Ferromagnetic bcc iron

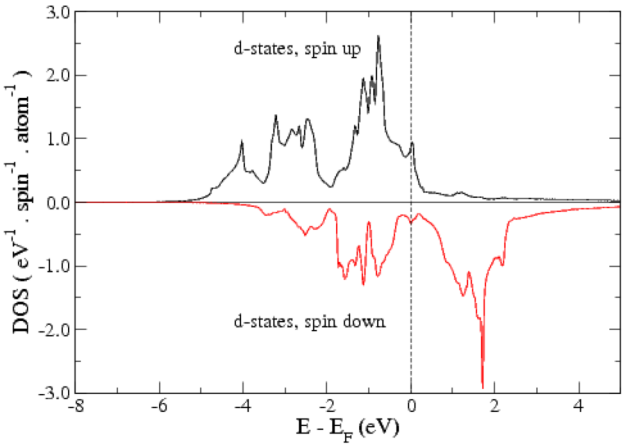

Expt: Photoemission

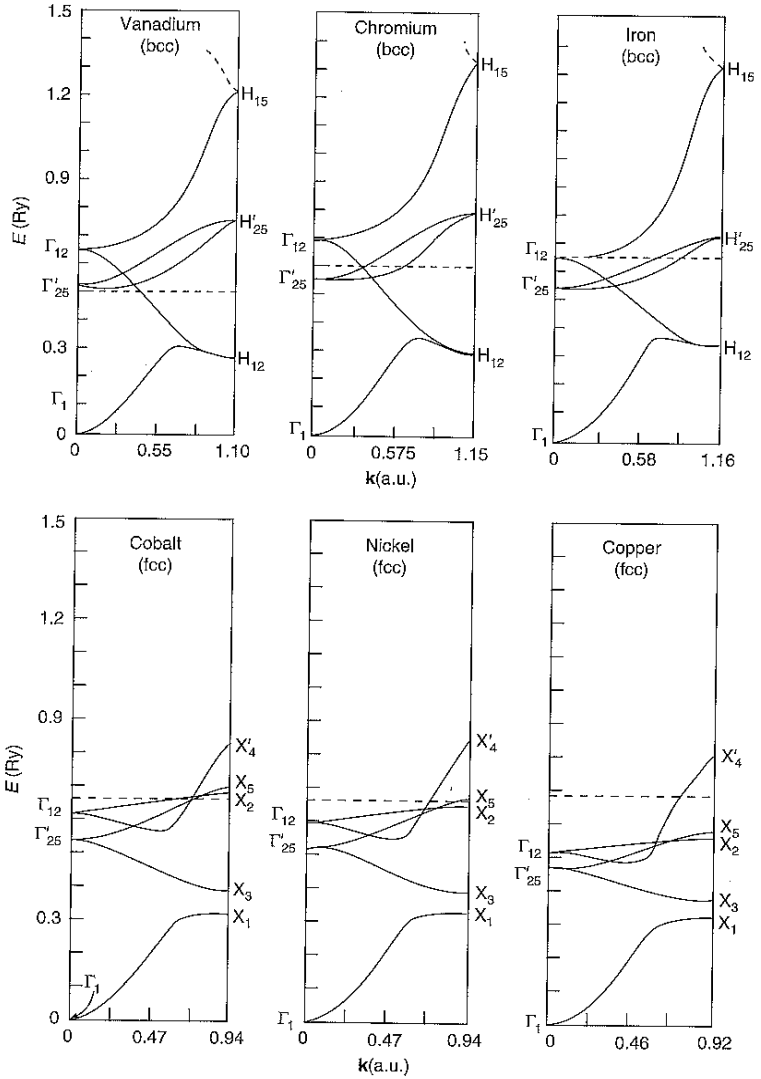

Figure 16.4. Bands of 3d metals showing the narrow d bands crossing the wide s band, and the progression of band filling across transition series. Calculations were done by Mattheiss [646] usin the APW method.

Bloch spectral function $A_{\mathrm{B}}(\vec{k}, E)$ of $Fe_{0.2}Ni_{0.8}$
for $\vec{k}$ along $\Gamma - X$

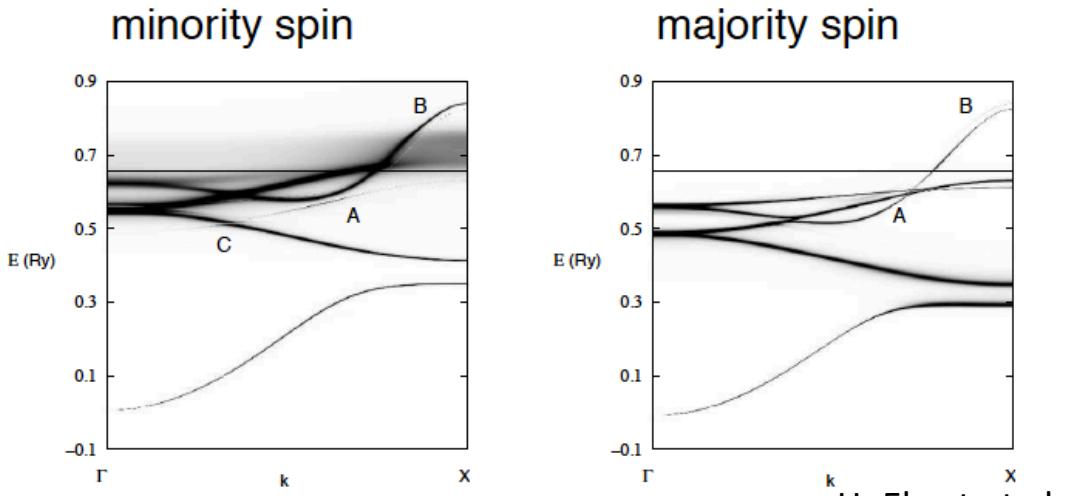

H. Ebert et al.

Angle resolved photoemission spectroscopy (ARPES)

Graphene band structures (experiment & theory)

PRL **98**, 206802 (2007)

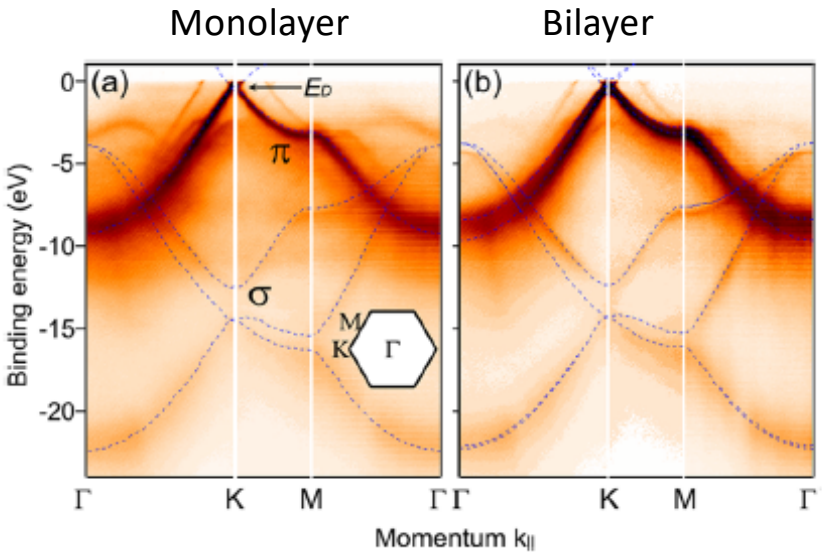

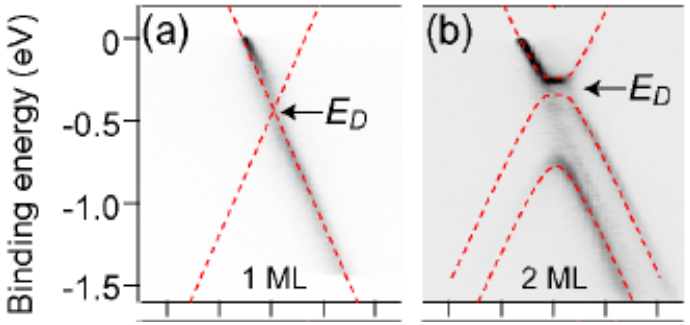

Blue line: theory (tight binding)

red line: theory (tight binding)

Valence band photoemission spectroscopy

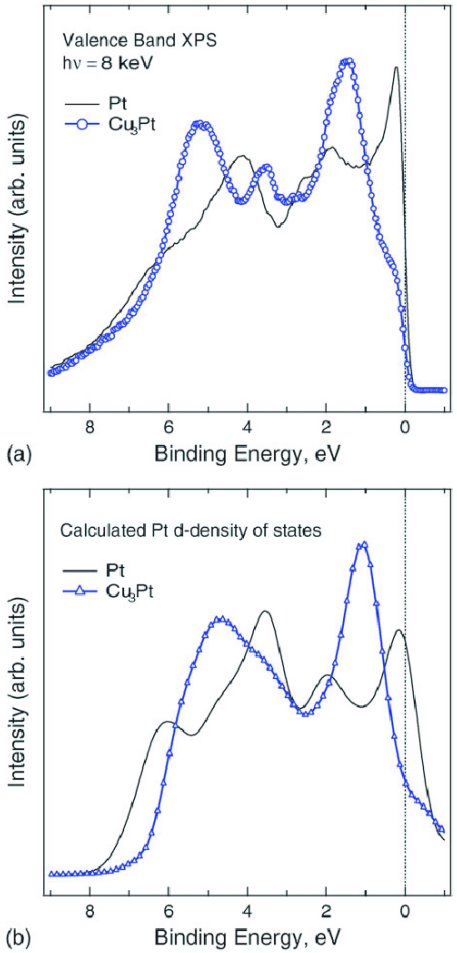

PCCP **12**, 5694 (2010)

PRB **58**, 9817 (1998)

BIS: Bremsstrahlung isochromat spectroscopy

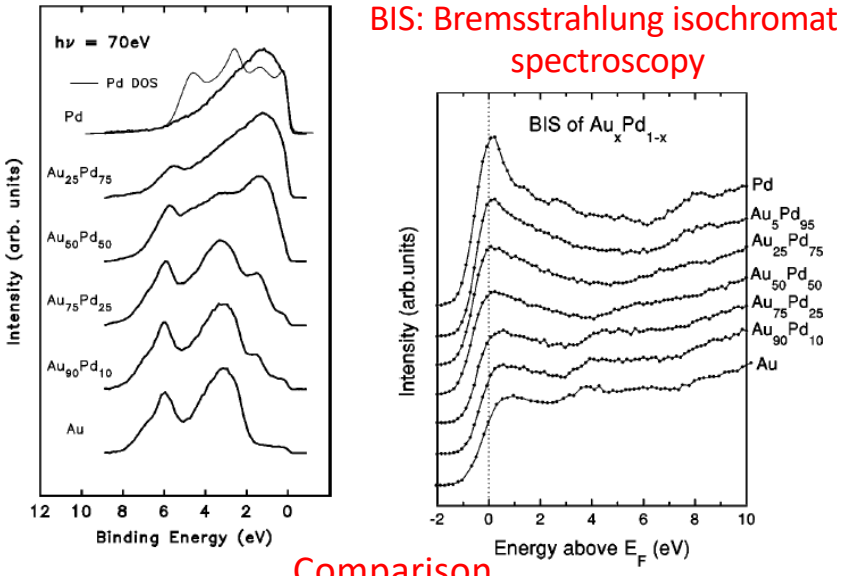

Comparison